


# Radiotherapy of Hodgkin and Non-Hodgkin Lymphoma: A Nonrigid Image-Based Registration Method for Automatic Localization of Prechemotherapy Gross Tumor Volume

Technology in Cancer Research & Treatment  
 2016, Vol. 15(2) 355–364  
 © The Author(s) 2015  
 Reprints and permission:  
[sagepub.com/journalsPermissions.nav](http://sagepub.com/journalsPermissions.nav)  
 DOI: 10.1177/1533034615582290  
[tct.sagepub.com](http://tct.sagepub.com)  


P. Zaffino, MSc<sup>1</sup>, D. Ciardo, MSc<sup>2</sup>, G. Piperno, MD<sup>2</sup>, L. L. Travaini, MD<sup>3</sup>,  
 S. Comi, MSc<sup>4</sup>, A. Ferrari, MD<sup>2</sup>, D. Alterio, MD<sup>2</sup>, B. A. Jereczek-Fossa, PhD, MD<sup>2,5</sup>,  
 R. Orecchia, MD<sup>2,5,6</sup>, G. Baroni, PhD<sup>7,8</sup>, and M. F. Spadea, PhD<sup>1</sup>

## Abstract

**Purpose:** To improve the contouring of clinical target volume for the radiotherapy of neck Hodgkin/non-Hodgkin lymphoma by localizing the prechemotherapy gross target volume onto the simulation computed tomography using [<sup>18</sup>F]-fluorodeoxyglucose positron emission tomography/computed tomography. **Material and Methods:** The gross target volume delineated on prechemotherapy [<sup>18</sup>F]-fluorodeoxyglucose positron emission tomography/computed tomography images was warped onto simulation computed tomography using deformable image registration. Fifteen patients with neck Hodgkin/non-Hodgkin lymphoma were analyzed. Quality of image registration was measured by computing the Dice similarity coefficient on warped organs at risk. Five radiation oncologists visually scored the localization of automatic gross target volume, ranking it from 1 (wrong) to 5 (excellent). Deformable registration was compared to rigid registration by computing the overlap index between the automatic gross target volume and the planned clinical target volume and quantifying the V<sub>95</sub> coverage. **Results:** The Dice similarity coefficient was  $0.80 \pm 0.07$  (median  $\pm$  quartiles). The physicians' survey had a median score equal to 4 (good). By comparing the rigid versus deformable registration, the overlap index increased from a factor of about 4 and the V<sub>95</sub> (percentage of volume receiving the 95% of the prescribed dose) went from  $0.84 \pm 0.38$  to  $0.99 \pm 0.10$  (median  $\pm$  quartiles). **Conclusion:** This study demonstrates the impact of using deformable registration between prechemotherapy [<sup>18</sup>F]-fluorodeoxyglucose positron emission tomography/computed tomography and simulation computed tomography, in order to automatically localize the gross target volume for radiotherapy treatment of patients with Hodgkin/non-Hodgkin lymphoma.

## Keywords

neck lymphoma, GTV identification, [<sup>18</sup>F]FDG-PET/CT radiation planning, deformable registration

## Abbreviations

[<sup>18</sup>F]FDG-PET/CT, [<sup>18</sup>F]-Fluorodeoxyglucose Positron Emission Tomography/Computed Tomography; CMT, combined modality treatment; CT, computed tomography; CTV, clinical target volume; DSC, Dice similarity coefficient; EFRT, extended field radiation therapy; FDG, fluorodeoxyglucose; GTV, gross tumor volume; NHL, non-Hodgkin lymphoma; HL, Hodgkin lymphoma; IFRT, involved field radiation therapy; INRT, involved node radiation therapy; OARs, organs at risk; OI, overlap index; PTV, planning target volume; RT, radiation therapy; TLI/TNI, total lymphoid/nodal irradiation. IA, stage I, subclassification A; IEA, stage IE, subclassification A; IIIs, stage III included spleen.

Received: December 2, 2014; Revised: March 9, 2015; Accepted: March 19, 2015.

<sup>1</sup> Department of Experimental and Clinical Medicine, Magna Graecia University, Catanzaro, Italy

<sup>2</sup> Department of Radiation Oncology, European Institute of Oncology, Milano, Italy

<sup>3</sup> Nuclear Medicine Division, European Institute of Oncology, Milan, Italy

<sup>4</sup> Medical Physics Unit, European Institute of Oncology, Milano, Italy

<sup>5</sup> Department of Health Sciences, Università degli Studi di Milano, Milano, Italy

<sup>6</sup> Centro Nazionale di Adroterapia Oncologica, Pavia, Italy

<sup>7</sup> Dipartimento di Elettronica, Informazione e Bioingegneria, Politecnico di Milano, Milano, Italy

<sup>8</sup> Bioengineering Unit, Centro Nazionale di Adroterapia Oncologica, Pavia, Italy

## Corresponding Author:

P. Zaffino, MSc, Department of Experimental and Clinical Medicine, Magna Graecia University, Catanzaro, Italy.

Email: [p.zaffino@unicz.it](mailto:p.zaffino@unicz.it)

## Introduction

The common clinical practice to treat limited stage (Ann Arbor I and II stage) lymphoma disease consists of a variable number of chemotherapy cycles followed by radiation therapy (RT).<sup>1-5</sup> For the early-stage Hodgkin lymphoma (HL) and Non-HL (NHL), the combined modality treatment (CMT) has shown higher patient survival and better local tumor control.<sup>6,7</sup>

Staging is performed by physical examination, blood test, and tomographic imaging (usually computed tomography [CT] preferably coupled with [<sup>18</sup>F]-fluorodeoxyglucose positron emission tomography [<sup>18</sup>F]FDG-PET), which provides anatomical and metabolic information about the lymph nodes involved. After chemotherapy is selected and delivered, lymph nodes usually shrink and postchemotherapy imaging might show just residual active regions or might be totally negative. However, current guidelines for CMT indicate that the affected primitive regions need to be treated with RT.<sup>8</sup> So the correct identification of the volume to be irradiated is fundamental.

Both chemotherapy and radiotherapy can lead to severe late side effects, including second malignancy, heart disease, thyroid dysfunction, sterility, gastritis, enteritis, pneumonitis, and so on.<sup>9,10</sup> Therefore, over the last few years, the trend is to reduce the aggressiveness of the treatments. More specifically, the tendency in RT is to reduce the dose and the volume of tissue to be treated,<sup>11-14</sup> thus being very precise and specific. Ranging from the largest to the smallest size of the irradiated region, RT treatments can be classified as total lymphoid/nodal irradiation (TLI/TNI), extended field RT (EFRT), extensive mantle field, involved field RT (IFRT), and involved node RT (INRT). Nowadays, TNI and the EFRT are mostly abandoned, and common treatments are IFRT, if the RT field encompasses all of the clinically involved regions and INRT, which envisages delivering the dose on the initially involved nodes, rather than on the whole nodal chain area.<sup>12,15,16</sup> For both IFRT and INRT, the prechemotherapy gross tumor volume (GTV) provides the reference for determining the clinical target volume (CTV). The smaller is the target to be irradiated, the more important is to delineate the CTV precisely.<sup>14</sup> Recent studies proved high observer variability in tumor delineation for HL,<sup>17-19</sup> thus highlighting the need of a robust and operator-independent methodology for target definition. A considerable improvement in treatment volume definition on simulation CT has been obtained by integrating the information provided by the [<sup>18</sup>F]FDG-PET/CT, acquired before chemotherapy for diagnosis and staging purposes.<sup>4,5,13,14,16,20-23</sup>

In order to combine the [<sup>18</sup>F]FDG-PET/CT outcome with the CT-based CTV delineation, the common routine is visual assessment: The physician compares the two imaging modalities, displayed on 2 different screens, and grounds the matching on anatomical landmarks. However, this approach is time consuming and operator dependent. Some authors proposed methods based on image rigid coregistration and overlay (image fusion) and highlighted more favorable results if the [<sup>18</sup>F]FDG-PET/CT scan is acquired on patients in treatment position.<sup>13,16,24</sup>

However, in most cases, patients are scanned in different setup (position of the arms and/or neck) and/or using different scanners in different hospitals. In addition, weight loss and lymph node shrinkage occurring between the 2 imaging stages represent particularly challenging issues for CT-[<sup>18</sup>F]FDG-PET/CT matching based on rigid registration.

In this work, we propose a new methodology to overcome these limitations by using nonrigid image registration between diagnostic [<sup>18</sup>F]FDG-PET/CT and simulation CT images. This approach can be useful in most clinical situations, regardless of the specific imaging setup/acquisition protocol and the chemotherapy outcome. To our knowledge, this is the first study demonstrating the use of deformable image registration as a technique to map the initial involved lymph node regions onto the radiotherapy images.

We tested our method on a cohort of patients treated for neck HL or NHL disease. Data analysis also included the comparison between rigid and nonrigid registration. The ultimate aim is to provide clinicians with robust guidance during the contouring phase, for speeding up the planning phase and improving the treatment efficacy by identifying accurately the primary lesion on the simulation CT scans.

## Materials and Methods

### Clinical Protocol and Patients

We selected retrospectively 15 patients treated at the European Institute of Oncology in Milan (Italy) for neck lymphoma. In particular, 5 of them were diagnosed with HL and 10 with NHL. In all, 13 patients were treated with CMT and 2 patients refused chemotherapy and underwent RT only. Details about each patient, regarding diagnosis, staging, imaging setup, and radiotherapy treatment are included in Table 1.

The institutional clinical protocol for CMT of lymphoma is as follows:

- Prechemotherapy [<sup>18</sup>F]FDG-PET/CT (Discovery, GE Medical Systems, Milwaukee, Wisconsin) is acquired for diagnosis and staging purposes.
- Image readout is performed on a Xeleris Workstation (GE Medical Systems, Milwaukee Wisconsin), which allows visualizing [<sup>18</sup>F]FDG-PET, CT and fused [<sup>18</sup>F]FDG-PET/CT sections in transverse, coronal, and sagittal planes. [<sup>18</sup>F]FDG-PET/CT images are interpreted by an experienced nuclear medicine physician (informed about the clinical and the radiological findings of the case), in collaboration with an experienced radiation oncologist. The presence of pathological FDG uptake to define the GTV is indicated when tracer uptake increases with respect to surrounding tissues and normal structures. The nuclear medicine physician always checks the anatomical correspondence of the FDG target on CT images, since patient's random or physiological movements can cause image mismatch.

**Table 1.** Patients' CT Information.<sup>a</sup>

Patient	Diagnosis	Stage	Neck Position Between CT <sub>DIAGN</sub> and CT <sub>SIM</sub>	Arms Position Between CT <sub>DIAGN</sub> and CT <sub>SIM</sub>	Time Interval Between CT <sub>DIAGN</sub> and CT <sub>SIM</sub>	Radiotherapy Dose to PTV, Gy
1	NHL	IAE	Different	Similar	4 months	30.6
2	NHL	IAE	Similar	Different	2 months	30.6
3	NHL	IA	Similar	Similar	3 months	30.6
4	NHL	IIA	Different	Similar	5 months	30.6
5	NHL	IA	Similar	Different	3 months	30.6
6	NHL	IIA	Different	Different	4 months	30.6
7	HL	IA	Different	Different	4 months	30.6
8	HL	IA	Different	Different	3 months	30.6
9	NHL	IA	Different	Different	1 month	30
10	HL	IA	Different	Similar	4 months	30.6
11	NHL	IA	Different	Different	6 months	30
12	NHL	IEA	Different	Different	6 months	30.6
13	HL	IIIs	Similar	Similar	8 months	30
14 *	HL	recurrence	Similar	Different	8 days	20
15 *	NHL	IIA	Different	Different	1 day	20

Abbreviations: CT, computed tomography; [<sup>18</sup>F]FDG-PET, [<sup>18</sup>F]-fluorodeoxyglucose positron emission tomography; HL, Hodgkin lymphoma; NHL, non-Hodgkin lymphoma; PTV, planning target volume; IA, stage I, subclassification A; IEA, stage IE, subclassification A; IIIs, stage III included spleen.

<sup>a</sup>CT<sub>DIAGN</sub> and CT<sub>SIM</sub> are, respectively, the first diagnostic [<sup>18</sup>F]FDG-PET/CT and the radiotherapy simulation CT. Patients received radiotherapy only.

- Depending on diagnosis and stage, 2 to 4 cycles of chemotherapy are delivered to the patient.
- Postchemotherapy [<sup>18</sup>F]FDG-PET/CT is acquired to assess the response to treatment.
- A simulation CT (HiSpeed CT/I, GE Medical Systems) is acquired in a standardized position for the planning of the RT treatment, after the manufacturing of a thermo-plastic mask for patient immobilization with both arms along the body and hyperextended neck position.
- The radiation oncologist draws the GTV on the simulation CT by visually examining the first [<sup>18</sup>F]FDG-PET/CT; in case of partial response after chemotherapy (presence of pathological FDG uptake on the postchemotherapy [<sup>18</sup>F]FDG-PET/CT the residual mass is also contoured to receive a boost dose.
- Starting from GTV, the CTV is defined according to IFRT guidelines to include tissues that could host cancerous cells, although they do not show morphological or functional variations. Finally, a geometric isotropic margin of 1 cm is added to compensate setup errors and organ motion, for planning target volume definition.
- Usually, 3-dimensional (3D) conformal radiotherapy is applied for patient treatment; if the patient is a recurrence case, intensity-modulated RT is preferred.

register the CT<sub>DIAGN</sub> onto CT<sub>SIM</sub>. Before image registration, image histograms were stretched in order to enhance the soft tissues contrast. Histogram modification was performed using a piecewise linear function remapping intensity landmarks from (−1000, −800, −100, 0, 50, 100, 1000, 3071) to (−800, −800, −400, 0, 600, 800, 1000, 1000). Since the stretched image highlights soft tissues at the expense of the dense ones, the processed CT was added to the original CT, in order to increase the contrast of both soft tissues and bones. This process was applied to each couple CT<sub>DIAGN</sub>-CT<sub>SIM</sub>. A multistage iterative B-spline-based registration procedure, minimizing the sum of squared voxel differences, was run for image registration. The registration process consisted of a rigid alignment followed by 4 deformable stages, going from coarse to fine registration by means of a progressive reduction in B-spline grid tile. The Plastimatch configuration file is provided in Appendix A. The registration output was a vector field describing the voxel displacements from CT<sub>DIAGN</sub> to CT<sub>SIM</sub>.

For validation purposes, we asked the radiation oncologist to contour on CT<sub>DIAGN</sub> organs at risk (OARs) typically included in the radiotherapy plan, such as parotid glands, spinal cord, trachea, larynx, and mandible (OAR<sub>DIAGN</sub>). The CTV and OARs were already available on the CT<sub>SIM</sub> (OAR<sub>SIM</sub>). The OAR<sub>DIAGN</sub> and GTV (identified as stated in the clinical protocol, 'Clinical Protocol and Patients' section) were warped according to the output vector field, obtaining OAR<sub>DIAGN\_WARPED</sub> and GTV<sub>DIAGN\_WARPED</sub>. In order to compare the impact of rigid versus deformable registration, the GTV volume after rigid alignment was also computed (GTV<sub>DIAGN\_RIGID</sub>). The algorithm was executed on a GNU/Linux workstation equipped with an Intel Xeon CPU 2.5 GHz and 8 GB of random access memory, requiring approximately a computation time of up to 8 minutes.

## Methodology

Figure 1 depicts the workflow of the methodology proposed in this study. The CT volume obtained by the first diagnostic [<sup>18</sup>F]FDG-PET/CT acquisition and the simulation CT were used as input data. We will refer to them as CT<sub>DIAGN</sub> and CT<sub>SIM</sub>, respectively. An open source registration software (Plastimatch; www.plastimatch.org)<sup>25,26</sup> was employed to

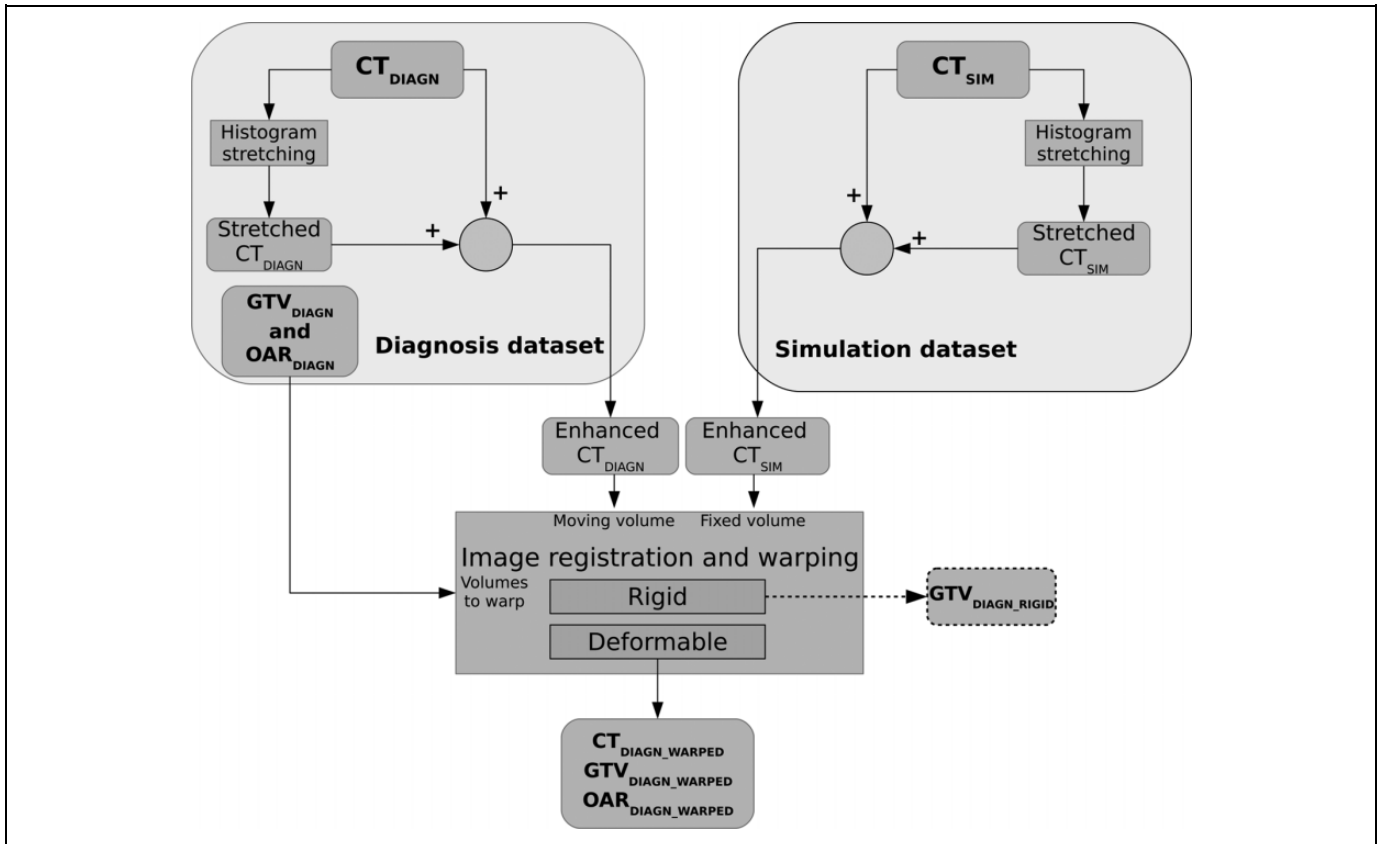


**Figure 1.** Flowchart of the proposed methodology. Dotted paths represent activities carried out for testing purposes.

### Data Analysis

**Image registration.** Image registration outcome was assessed by quantitatively comparing each  $OAR_{DIAGN\_WARPED}$  with the corresponding  $OAR_{SIM}$  (representing the ground truth). The Dice similarity coefficient (DSC)<sup>27</sup> was calculated for each couple  $OAR_{DIAGN\_WARPED}/OAR_{SIM}$  according to the following formula:

$$DSC = \frac{2|OAR_{DIAGN\_WARPED} \cap OAR_{SIM}|}{OAR_{DIAGN\_WARPED} + OAR_{SIM}} \quad (1)$$

DCS value was interpreted as a function of the structure volume, as described in Isambert *et al.*<sup>28</sup>

**$GTV_{DIAGN\_WARPED}$  Localization.** Five radiation oncologists were asked to visually score the quality of  $GTV_{DIAGN\_WARPED}$  location on the  $CT_{SIM}$ . By using 2 different screens, each rater was presented simultaneously with the original  $GTV$  onto  $CT_{DIAGN}$  and with the  $GTV_{DIAGN\_WARPED}$  onto  $CT_{SIM}$ . Their task was to evaluate whether or not the  $GTV_{DIAGN\_WARPED}$  was correctly localized on the  $CT_{SIM}$  based on its relative spatial localization with respect to the neighbor soft tissues and landmark anatomical structures (eg, bones and organs). Scores ranged from 1 to 5, being 1 = wrong, 2 = poor, 3 = fair, 4 = good, and 5 = excellent. The median score for each patient was computed as final grade for  $GTV_{DIAGN\_WARPED}$ .

Finally, deformable and rigid registration outcomes were compared from both geometric and dosimetric point of view by computing the overlap index (OI), that is, the percentage of  $GTV_{DIAGN\_WARPED}$  (or  $GTV_{DIAGN\_RIGID}$ ) included in the planned CTV (Equation 2)

$$OI_x = \frac{|GTV_x \cap CTV|}{GTV}, \quad (2)$$

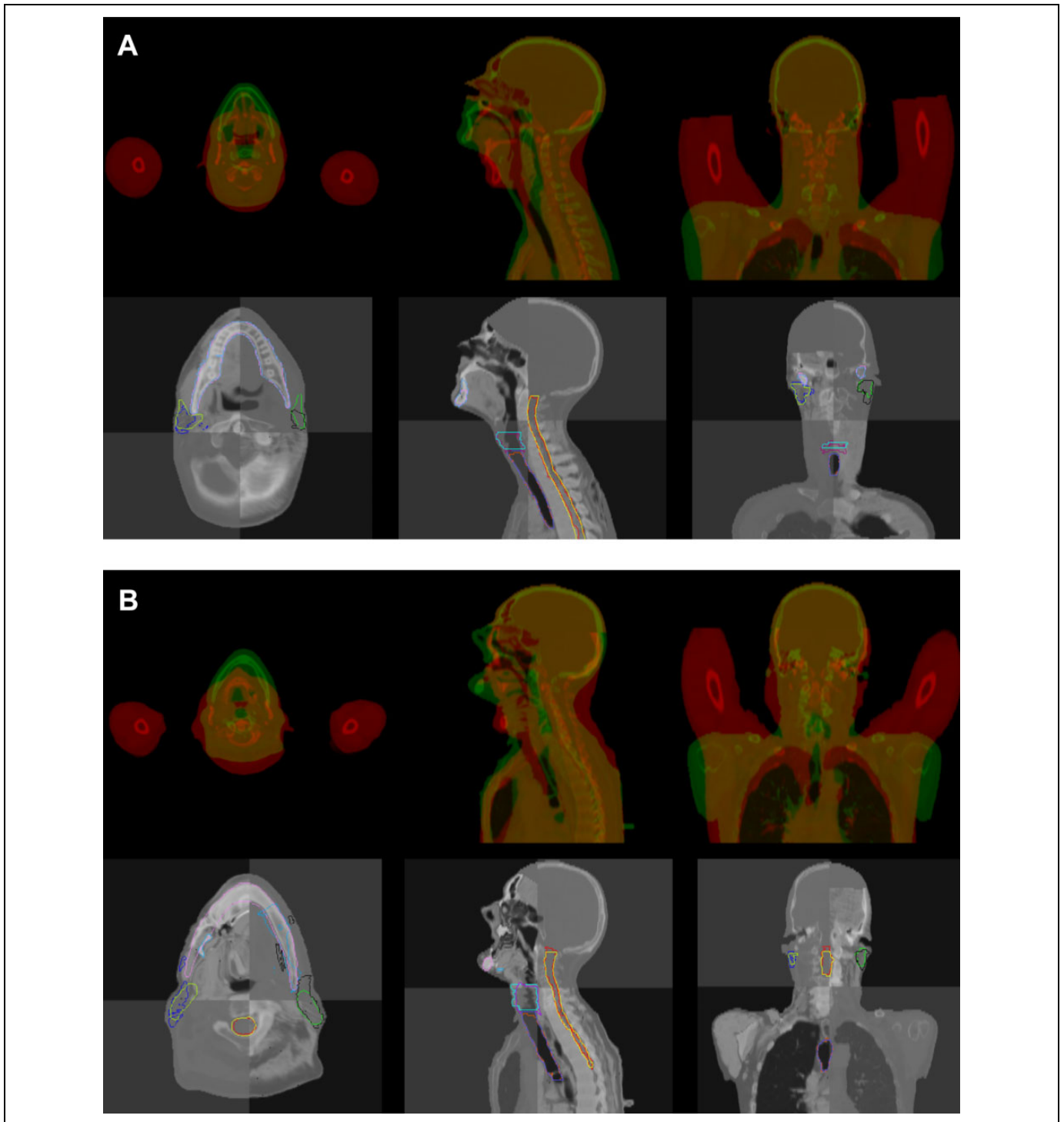
with  $x = DIAGN\_WARPED$  or  $x = DIAGN\_RIGID$ , and the volume of  $GTV_{DIAGN\_WARPED}$  and  $GTV_{DIAGN\_RIGID}$  receiving the 95% of nominal dose ( $V_{95}$ ). Dosimetric analysis was performed by SlicerRT (<http://slicerrt.github.io>),<sup>29</sup> a plugin of 3D Slicer ([www.slicer.org](http://www.slicer.org)).<sup>30</sup> The Wilcoxon test was chosen to verify whether statistical difference existed between paired samples coming from a data distribution not strictly Gaussian.

### Results

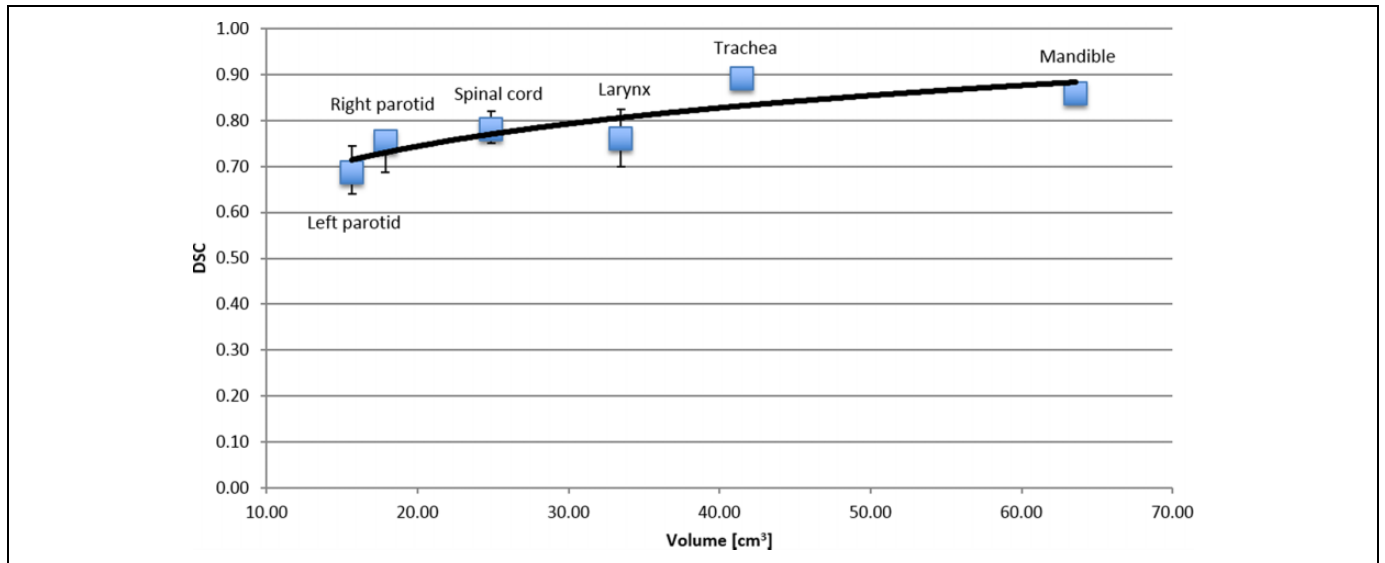
The time interval occurring between diagnostic and treatment planning scans ranged from 8 months to 1 day, with a median value of 4 months.

Figure 2 shows 2 representative cases of a good (patient 8) and a bad (patient 7) image registration result.

Figure 3 shows the median  $\pm$  quartiles of DSC as a function of structure's median volume. Best results were found for



**Figure 2.** An example of good (A) and bad (B) image registration. In (A) and (B) the  $CT_{DIAGN}$  (red) is overlaid to  $CT_{SIM}$  (green) to show the initial situation while, later, the  $CT_{SIM}$ , the  $CT_{DIAGN\_WARPED}$  and the  $OAR_{SIM}/OAR_{DIAGN\_WARPED}$  are depicted in checkerboard mode with a different histogram window to improve the visualization of the result. In (A), anatomical landmarks between  $CT_{SIM}$  and  $CT_{DIAGN\_WARPED}$ , at the edge of each checker box, match; the warped OARs are consistently overlaid on the original ones. In (B), the  $CT_{DIAGN\_WARPED}$ , depicted in the upper left and in the lower right checker boxes, present unnatural swirls due to excessive distortion of the b-spline grid; as a consequence, the warped OARs are broken into small islands, such as mandible (in light blue), right and left parotid (in black and dark blue respectively).



**Figure 3.** Organs at risk (OARs): logarithmic correlation between Dice similarity coefficient (DSC) and volume.

**Table 2.** Physicians’ Scores of GTV Localization on CT<sub>SIM</sub>.

Rater	Patient														
	1	2	3	4	5	6	7	8	9	10	11	12	13	14	15
#1	4	4	5	2	5	2	2	4	1	5	1	5	5	4	3
#2	4	4	4	4	4	5	3	4	5	4	3	3	4	4	4
#3	4	4	4	3	4	3	1	4	4	4	3	5	4	5	4
#4	3	4	4	4	3	4	4	4.5	4	5	2	2	1	3	4
#5	4	4	5	5	3	4	3	3	5	5	4	4	5	4	4
Median	4	4	4	4	4	4	3	4	4	5	3	4	4	4	4

Abbreviation: GTV, gross tumor volume.

mandible ( $0.86 \pm 0.02$ ) and trachea ( $0.89 \pm 0.02$ ), and worst outcomes were obtained for right ( $0.69 \pm 0.05$ ) and left ( $0.75 \pm 0.04$ ) parotid and for larynx ( $0.76 \pm 0.05$ ). Spinal cord scored  $0.78 \pm 0.03$ . The DSC plotted versus volume showed an increasing trend, fitting a logarithmic curve at 95% prediction bounds ( $R^2 = 0.72$ ). Among all, larynx and trachea exhibited the most discordant behavior from the fitting, being y-residual  $-0.05$  and  $+0.06$ , respectively.

In Table 2, the results of the performed survey are reported. Besides a general good performance of the algorithm reported by physicians (median  $\pm$  quartiles:  $4 \pm 0.5$ ), 2 of 15 cases were indicated as just sufficient (see patients 7 and 11), with median score equal to 3. In 2 circumstances, 1 rater largely disagreed with the others by underrating the outcome of the algorithm (see patients 9 and 13).

The comparison between rigid and deformable registration is reported in Figure 4. Median  $\pm$  quartiles for OI were  $0.21 \pm 0.16$  (rigid) and  $0.74 \pm 0.13$  (deformable), and for  $V_{95}$ , were  $0.84 \pm 0.38$  (rigid) and  $0.99 \pm 0.10$  (deformable). Wilcoxon matched-pair test, performed at 5% confidence level, revealed statistical difference both for  $OI_{DIAGN\_RIGID}$  versus  $OI_{DIAGN\_WARPED}$  ( $p < 10^{-5}$ ) and for  $V_{95\_DIAGN\_RIGID}$  versus  $V_{95\_DIAGN\_WARPED}$  ( $P = .005$ ).

In Figure 4, a comparison between rigid and deformable registration in terms of GTV localization, dosimetric coverage and OI, and  $V_{95}$  is depicted.

### Discussion

In this work, we described an image-based methodology to improve the delineation of the CTV for RT treatment of neck HL and NHL. Our approach was based on mapping the GTV, extracted from the diagnostic  $[^{18}\text{F}]\text{FDG-PET/CT}$ , onto the simulation CT volume, by means of nonrigid image registration.

Other investigators proposed to use rigid image registration to integrate the  $[^{18}\text{F}]\text{FDG-PET/CT}$  information with the simulation CT data set.<sup>13,16,24</sup> However, in those studies they recommend to acquire the diagnosis and the treatment planning image data sets with similar patient positioning and, possibly, with the same devices for patient setup and immobilization. Conversely, we enrolled patients who were scanned in different position (arms and neck particularly), in order to test the method in the most challenging circumstances.

Image registration was performed only between CT volumes that, by offering better anatomical detail compared to  $[^{18}\text{F}]\text{FDG-PET}$  imaging, guarantee a more reliable result. The  $[^{18}\text{F}]\text{FDG-PET}$ , coregistered by hardware to  $\text{CT}_{DIAGN}$ , was used to contour the GTV, according to the clinical protocol. The image registration algorithm was executed by setting the same parameters (metric, number of stages, B-spline grid, number of iterations, optimizer, etc) for all patients. This choice was motivated by the fact that in a clinical environment, the system must be stable and robust. The parameters were tested and chosen on the basis of previous studies.<sup>31,32</sup> The choice to gradually reduce the B-spline grid tile was made in order to level first the macroscopic differences and then the finer ones. This strategy allows at the same time to avoid local minima

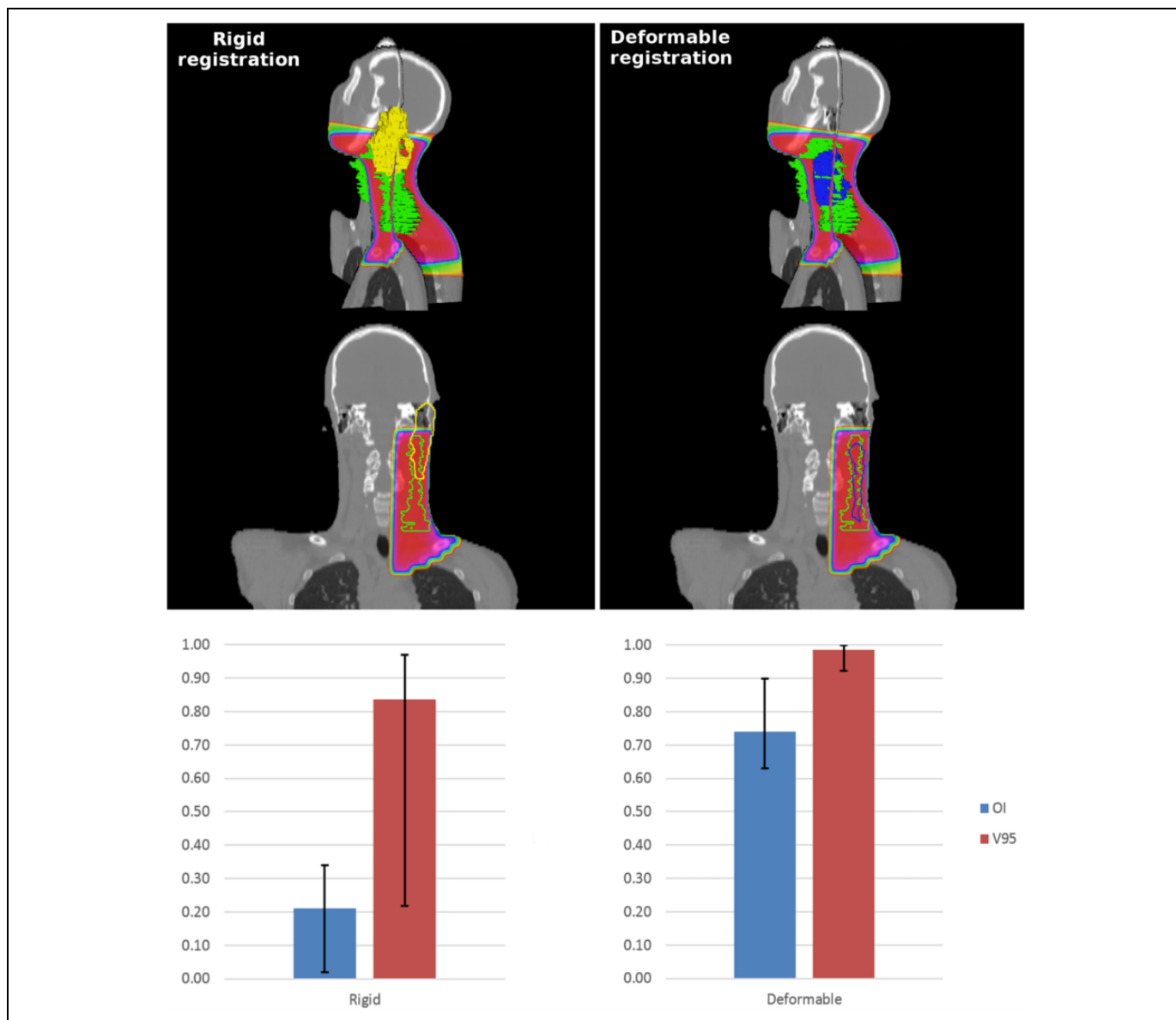


**Figure 4.** Patient 8’s CT<sub>SIM</sub>, dose and contours. The left panel shows the result of the rigid alignment (clinical target volume [CTV] green, GTV<sub>DIAGN\_RIGID</sub> yellow); in the right panel is depicted the result of the deformable registration (CTV green, GTV<sub>DIAGN\_WARPED</sub> blue). At the bottom is the comparison between rigid and deformable registration in terms of overlap index (OI) and V<sub>95</sub>.

during the searching of the optimal transformation. For the same reasons, and to speed up the process, the rigid transformation was computed by subsampling the images.

The quality of image registration was assessed by computing the DSC between reference OAR<sub>SIM</sub> and warped OAR<sub>DIAGN\_WARPED</sub>. The median ± quartiles values of DSC ranged from 0.69 ± 0.05 to 0.89 ± 0.02. Mandible, spinal cord, and trachea exhibited the highest values, while parotids the lowest. This is not surprising since parotid glands are very difficult to contour and have large intra and inter-rater variability.<sup>33</sup> Moreover, we found a logarithmic correlation between volume size and DSC, in agreement with Isambert *et al.* who showed that the smaller a structure is the more the DSC is affected by mislabeling a small number

of voxels.<sup>28</sup> Larynx DSC exhibited lower values compared to the expected ones and the highest variability. This is due to the fact that in all those patients where the neck position significantly differed between CT<sub>DIAGN</sub> and CT<sub>SIM</sub> (10 cases), larynx was the structure that was mostly affected by different setups. Conversely, trachea value was higher than expected because it turned out to be less influenced by neck, mandible, or arm positions. When envisioning a future clinical scenario, it would be recommendable to delineate mandible, larynx, and spinal cord on the CT<sub>DIAGN</sub> as a way to critically evaluate the registration process. No correlation was found between the interscan time and the final registration outcome. Local misregistration mainly occurred in the shoulder region when arms’ position was

different between  $CT_{DIAGN}$  and  $CT_{SIM}$ . In only 2 cases (patients 7 and 11), the dissimilar neck elongation caused irregular registration in the mandible area.

When evaluating the  $GTV_{DIAGN\_WARPED}$  localization, the lowest median score was 3 (“fair”), and it occurred in 2 of 15 cases. In both cases, deformable registration did not perform well in the neck region as highlighted by the median DSC for each patient (0.78 and 0.63, respectively), being the lowest among the entire patient cohort. This caused an irregular warping of the  $GTV_{DIAGN\_WARPED}$  that was not judged fully acceptable by most of the raters. Compared to rigid alignment, deformable image registration is more affected by metal artifact effects. This is due to the fact that the displacement field is computed locally, unlike the rigid transformation where it is computed on the whole volume. However, we found that mild misregistration due to metal artifacts (5 cases in our data set) did not affect the final warping and localization of the GTV. When metal artifacts are a concern, algorithms for their reduction should be used in order to mitigate the problem.

As far as the comparison between rigid and deformable registration is concerned, both OI and  $V_{95}$  showed statistical difference. Although on a limited data set, the overall results showed that deformable registration performs better than rigid registration. This is due to the fact that we enrolled patients acquired in very different arms/neck position during the diagnosis and simulation CT. This large difference cannot be recovered by using only a rigid alignment but requires a deformable image registration approach. The gap between rigid and deformable registration was particularly evident for the OI. The  $V_{95}$  contrast was mitigated by the fact that IFRT was planned for these patients. We would expect higher differences, in favor of deformable registration, in case of INRT.

## Conclusion

In conclusion, the proposed methodology turned out to improve image-based guidance for the radiation oncologists during the CTV contouring of neck lymph nodes for patients with HL/NHL. In clinical practice, the described method is put forward as a valuable tool for reducing the CTV delineation variability and improve the primary disease localization.

## Appendix A

The complete list of Plastimatch registration parameters stages:

```
[STAGE]
xform=align_center
```

```
[STAGE]
xform=rigid
optim=versor
impl=itk
metric=mse
max_its=100
convergence_tol=5
grad_tol=1.5
```

```
res=4 4 2
[STAGE]
xform=bspline
optim=lbfgsb
impl=plastimatch
metric=mse
max_its=150
res=1 1 1
grid_spac=40 40 50
```

```
[STAGE]
xform=bspline
optim=lbfgsb
impl=plastimatch
metric=mse
max_its=100
res=1 1 1
grid_spac=20 20 30
```

```
[STAGE]
xform=bspline
optim=lbfgsb
impl=plastimatch
metric=mse
max_its=50
res=1 1 1
grid_spac=10 10 10
```

```
[STAGE]
xform=bspline
optim=lbfgsb
impl=plastimatch
metric=mse
max_its=50
res=1 1 1
grid_spac=5 5 5
```

## Acknowledgments

The authors thank the Doctors Mariaquila Santoro (Azienda ospedaliera “Pugliese-Ciaccio”, Catanzaro, Italy) and Giulia Marvaso (Medical Oncology Unit; Magna Graecia University of Catanzaro and T. Campanella Cancer Center, Catanzaro, Italy) for their contribution to visual scoring the automatic contours.

## Declaration of Conflicting Interests

The author(s) declared no potential conflicts of interest with respect to the research, authorship, and/or publication of this article.

## Funding

The author(s) received no financial support for the research, authorship, and/or publication of this article.

## References

- Engert A, Franklin J, Eich HT, *et al.* Two cycles of doxorubicin, bleomycin, vinblastine, and dacarbazine plus extended-field radiotherapy is superior to radiotherapy alone in early favorable



- Hodgkin's lymphoma: final results of the GHSG HD7 trial. *J Clin Oncol*. 2007;25(23):3495-3502.
2. Fermé C, Eghbali H, Meerwaldt JH, et al. Chemotherapy plus involved-field radiation in early-stage Hodgkin's disease. *N Engl J Med*. 2007;357(19):1916-1927. doi:10.1056/NEJMoa064601.
  3. Eich HT, Diehl V, Görgen H, et al. Intensified chemotherapy and dose-reduced involved-field radiotherapy in patients with early unfavorable Hodgkin's lymphoma: final analysis of the German Hodgkin Study Group HD11 trial. *J Clin Oncol*. 2010;28(27):4199-4206. doi:10.1200/JCO.2010.29.8018.
  4. Hoskin PJ, Díez P, Williams M, Lucraft H, Bayne M. Recommendations for the use of radiotherapy in nodal lymphoma. *Clin Oncol (R Coll Radiol)*. 2013;25(1):49-58. doi:10.1016/j.clon.2012.07.011.
  5. Specht L, Yahalom J, Illidge T, et al. Modern radiation therapy for Hodgkin lymphoma: field and dose guidelines from the International Lymphoma Radiation Oncology Group (ILROG). *Int J Radiat Oncol Biol Phys*. 2014;89(4):854-862. doi:10.1016/j.ijrobp.2013.05.005.
  6. Herbst C, Rehan FA, Brillant C, et al. Combined modality treatment improves tumor control and overall survival in patients with early stage Hodgkin's lymphoma: a systematic review. *Haematologica*. 2010;95(3):394-500. doi:10.3324/haematol.2009.015644.
  7. Yahalom J. Does radiotherapy still have a place in Hodgkin lymphoma? *Curr Hematol Malig Rep*. 2009;4(3):117-124. doi:10.1007/s11899-009-0017-2.
  8. Illidge T, Specht L, Yahalom J, et al. Modern radiation therapy for nodal non-Hodgkin lymphoma—target definition and dose guidelines from the International Lymphoma Radiation Oncology Group. *Int J Radiat Oncol Biol Phys*. 2014;89(1):49-58. doi:10.1016/j.ijrobp.2014.01.006
  9. Ng AK, Mauch PM. Late effects of Hodgkin's disease and its treatment. *Cancer J*. 2009;15(2):164-168. doi:10.1097/PPO.0b013e31819e30d7.
  10. Darby SC, Cutter DJ, Boerma M, et al. Radiation-related heart disease: current knowledge and future prospects. *Int J Radiat Oncol Biol Phys*. 2010;76(3):656-665. doi:10.1016/j.ijrobp.2009.09.064.
  11. Klimm B, Engert A. Combined modality treatment of Hodgkin's lymphoma. *Cancer J*. 2009;15(2):143-149. doi:10.1097/PPO.0b013e31819e31ba.
  12. Goda JS, Tsang RW. Involved field radiotherapy for limited stage Hodgkin lymphoma: balancing treatment efficacy against long-term toxicities. *Hematol Oncol*. 2009;27(3):115-122. doi:10.1002/hon.890.
  13. Terezakis SA, Hunt MA, Kowalski A, et al. [<sup>18</sup>F] FDG-positron emission tomography coregistration with computed tomography scans for radiation treatment planning of lymphoma and hematologic malignancies. *Int J Radiat Oncol Biol Phys*. 2011;81(3):615-622. doi:10.1016/j.ijrobp.2010.06.044.
  14. Girinsky T, van der Maazen R, Specht L, et al. Involved-node radiotherapy (INRT) in patients with early Hodgkin lymphoma: Concepts and guidelines. *Radiother Oncol*. 2006;79(3):270-277. doi:10.1016/j.radonc.2006.05.015.
  15. Bar Ad V, Paltiel O, Glatstein E. Radiotherapy for early-stage Hodgkin's lymphoma: a 21st century perspective and review of multiple randomized clinical trials. *Int J Radiat Oncol Biol Phys*. 2008;72(5):1472-1479. doi:10.1016/j.ijrobp.2008.08.026.
  16. Eich HT, Müller RP, Engenhart-Cabillic R, et al. Involved-node radiotherapy in early-stage Hodgkin's lymphoma. Definition and guidelines of the German Hodgkin Study Group (GHSG). *Strahlenther Onkol*. 2008;184(8):406-410.
  17. Genovesi D, Cèfaro GA, Vinciguerra A, et al. Interobserver variability of clinical target volume delineation in supra-diaphragmatic Hodgkin's disease. A multi-institutional experience. *Strahlenther Onkol*. 2011;187(6):357-366. doi:10.1007/s00066-011-2221-y.
  18. Lütendorf-Caucig C, Fotina I, Gallop-Evans E, et al. Multi-center evaluation of different target volume delineation concepts in pediatric Hodgkin's lymphoma. A case study. *Strahlenther Onkol*. 2012;188(11):1025-1030. doi:10.1007/s00066-012-0182-4.
  19. Shikama N, Oguchi M, Isobe K, et al. Quality assurance of radiotherapy in a clinical trial for lymphoma: individual case review. *Anticancer Res*. 2007;27(4C):2621-2625.
  20. Seam P, Juweid ME, Cheson BD. The role of FDG-PET scans in patients with lymphoma. *Blood*. 2007;110(10):3507-3516. doi: http://dx.doi.org/10.1182/blood-2007-06-097238.
  21. Song MK, Chung JS, Lee JJ, et al. Metabolic tumor volume by positron emission tomography/computed tomography as a clinical parameter to determine therapeutic modality for early stage Hodgkin's lymphoma. *Cancer Sci*. 2013;104(12):1656-1661. doi:10.1111/cas.12282.
  22. Yahalom J. Transformation in the use of radiation therapy of Hodgkin lymphoma: new concepts and indications lead to modern field design and are assisted by PET imaging and intensity modulated radiation therapy (IMRT). *Eur J Haematol*. 2005;75(s66):90-97. doi:10.1111/j.1600-0609.2005.00461.x.
  23. Hutchings M, Loft A, Hansen M, Berthelsen AK, Specht L. Clinical impact of FDG-PET/CT in the planning of radiotherapy for early-stage Hodgkin lymphoma. *Eur J Haematol*. 2007;78(3):206-212. doi:10.1111/j.1600-0609.2006.00802.x.
  24. Robertson VL, Anderson CS, Keller FG, et al. Role of FDG-PET in the definition of involved-field radiation therapy and management for pediatric Hodgkin's lymphoma. *Int J Radiat Oncol Biol Phys*. 2011;80(2):324-332. doi:10.1016/j.ijrobp.2010.02.002.
  25. Sharp G, Li R, Wolfgang J, et al. Plastimatch: an open source software suite for radiotherapy image processing. In *Proceedings of the XVI<sup>th</sup> International Conference on the use of Computers in Radiotherapy (ICCR), Amsterdam, Netherlands; June 2010*.
  26. Shackelford JA, Shusharina N, Verberg J, et al. Plastimatch 1.6: current capabilities and future directions. *Proc. MICCAI 2012 Image-Guidance and Multimodal Dose Planning in Radiation Therapy Workshop; October 2012*.
  27. Dice LR. Measures of the amount of ecologic association between species. *Ecology*. 1945;26(3):297-302.
  28. Isambert A, Dhermain F, Bidault F, et al. Evaluation of an atlas-based automatic segmentation software for the delineation of brain organs at risk in a radiation therapy clinical context.

- Radiother Oncol.* 2008;87(1):93-99. doi:10.1016/j.radonc.2007.11.030.
29. Pinter C, Lasso A, Wang A, Jaffray D, Fichtinger G. SlicerRT—Radiation therapy research toolkit for 3D Slicer. *Med Phys.* 2012;39(10):6332-6338. doi:10.1118/1.4754659.
30. Pieper S, Halle M, Kikinis R. 3D Slicer. *Proc IEEE Int Symp Biomed Imaging.* 2004;1:632-635. doi:10.1109/ISBI.2004.1398617.
31. Peroni M, Ciardo D, Spadea MF, *et al.* Automatic segmentation and online virtual CT in head-and-neck adaptive radiation therapy. *Int J Radiat Oncol Biol Phys.* 2012;84(3):e427-e433. doi:10.1016/j.ijrobp.2012.04.003.
32. Murphy K, van Ginneken B, Reinhardt JM, *et al.* Evaluation of registration methods on thoracic CT: the EMPIRE10 challenge. *IEEE Trans Med Imaging.* 2011;30(11):1901-1920. doi:10.1109/TMI.2011.2158349.
33. Nelms BE, Tomè WA, Robinson G, Wheeler J. Variations in the contouring of organs at risk test case from a patient with oropharyngeal cancer. *Int J Radiat Oncol Biol Phys.* 2012;82(1):368-378. doi:10.1016/j.ijrobp.2010.10.019.